Anisotropic Nanohybrids

DOI: 10.1002/anie.201005619

Tailored Anisotropic Magnetic Chain Structures Hierarchically Assembled from Magnetoresponsive and Fluorescent Components**

*Arlin Jose Amali, Padmanapan Saravanan, and Rohit Kumar Rana**

The development of methods for controlling the organization of functional objects at a nanometer scale to build larger objects is of fundamental and technological interest. The unique electronic, magnetic, and optical properties of nanomaterials will be best utilized when they are well integrated into larger devices.[1–5] A great deal of research is focused on such materials, particularly those with magnetic properties that can be exploited for the fabrication of ordered one-dimensional (1D) chainlike assemblies. Pertinent targets include the synthesis of materials that have desirable anisotropic properties for electronic and optical devices.[6–9] As this is a difficult task, different techniques have been employed including magnetic-field-induced (MFI) assembly,[10–16] electric or magnetic dipole–dipole interactions,[17–20] crystallographically specific orientation,[21] non-uniform stabilizer distribution,[22] templated synthesis[23,24] to produce 1D nanostructured materials. However, an elegant approach would be to construct 1D chains consisting of structurally intricate units and functions. Suitable methods are still required to prepare aligned structures from nanoparticles suspended in an aqueous medium and to allow multifunctional properties to be imparted into such directional structures in a way that allows these additional properties to evaluated and exploited.

Herein, we describe a method that provides opportunities for synthesizing materials that not only have a preferred 1D structure but that are also multifunctional. The strategy involves both designing and utilizing nanobuilding blocks to be linked together to generate aligned materials with anisotropic morphology and multifunctional properties. In the first step we assemble preformed nanoparticles (NPs) into a confined structure by using positively charged polypeptides as interparticle mediators while preserving the constituent nanoparticles' functional properties. We have shown that the cationic polypeptides can undergo counterion condensation to form spherical aggregates by ionic cross-linking with either certain multivalent counteranions or nanoparticles which are capped with anionic species.[25,26] The unique aggregation characteristics of these polycation–anion systems means that multiple nanoparticles can spontaneously assemble into microstructures.[27,28] We have further shown that functionalities can also be integrated to give catalytic and optical properties.[29,30] Herein, our approach is to use poly(L-lysine) (PLL) to cross-link with hydroxy pyrene trisulfonate (HPTS) and citrate-functionalized magnetic nanoparticles (MNPs) to afford magneto responsive fluorescent spheres (MFS). In a second step these spheres are magnetically aligned by virtue of magnetic dipole interactions to construct 1D anisotropic shapes.

HPTS is a pyrene-based molecule and has been proved to be a versatile probe molecule in both chemistry and biology.[31] The ability of HPTS, as an anionic multiple-point cross-linking center, to electrostatically bind cations on different polyelectrolyte chains[32] can impart fluorescent properties to the resulting hybrid structures. To incorporate magnetic properties, we use citrate-functionalized Fe_3O_4 magnetic nanoparticles (MNPs) so that the ionic interaction of citrate with PLL can enable the formation of spherical MNP aggregates. The MNPs, synthesized by a co-precipitation method, are fully characterized to ensure their structure and the presence of the citrate functional group (Supporting Information, Figure S1).[33,34]

Scheme 1 illustrates our method to include both magnetic and fluorescent functions into the microspheres. Simultaneous columbic interactions between positively charged amine groups of PLL and the negatively charged carboxy groups on

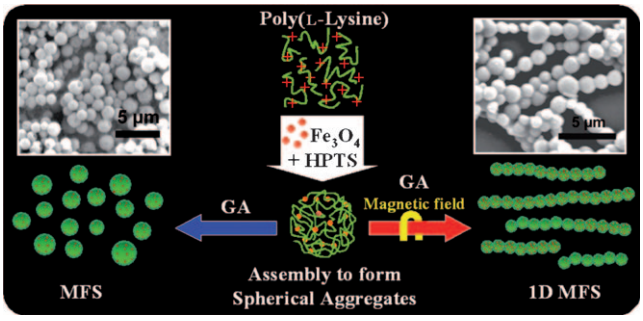

Scheme 1. Schematic illustration of the assembly of hydroxy pyrene trisulfonate (HPTS) and citrate-functionalized magnetic nanoparticles (MNPs) using poly(L-lysine) to generate magnetoresponsive fluorescent spheres (MFS; blue arrow). The same process in a magnetic field (red arrow) generates 1D structures exhibiting magnetic anisotropic properties. Insets: corresponding SEM images of MFS and 1D MFS. GA = glutaric dialdehyde.

[*] A. J. Amali, Dr. R. K. Rana
Nanomaterials Laboratory, I & PC Division
Indian Institute of Chemical Technology
Hyderabad 500 607 (India)
Fax: (+91) 40-2716-0921
E-mail: rkrana@iict.res.in
Dr. P. Saravanan
Defence Metallurgical Research Laboratory
Hyderabad 500 058 (India)

[**] Financial support from DST, India (SR/FTP/CS-72/2005), CSIR, India (NWP0035 and SRF), and DBT, India (BT/PR0010/NNT/28/87/2007) is acknowledged. We thank Dr. S. V. Manorama, N. Rangaraj, Dr. S. S. Madhavendra, and Dr. P. R. Bangal for their help in materials characterization.

Supporting information for this article is available on the WWW under http://dx.doi.org/10.1002/anie.201005619.

the citrate-stabilized MNPs and sulfonyl groups on HPTS, respectively, facilitate the MFS formation. The process is accompanied with spontaneous formation of a turbid solution and dynamic light-scattering (DLS) measurements give a clear indication that aggregates of sizes between 0.5–1.1 μm are produced (Supporting information, Figure S2). The sizes are similar to the aggregates formed between HPTS and PLL. This dynamic process based on the columbic interaction is sensitive to the reaction environment, such as temperature, pH value, and the ionic strength.[25–27] In our case, a pH value of approximately 7 ensures the presence of cationic ammonium groups in PLL ($pK_a \approx 11.0$), and anionic carboxylate and sulfate groups in citrate and HPTS, respectively. The interaction of polyamines with multivalent anions also depends on the charge ratio "R" and it has been observed that a ratio of $R > 1$ is required for the polymer aggregation to occur at similar concentrations.[25] At these ratios, addition of multivalent anions almost completely dissociates the monovalent anions (Br^-) from the polyamine side chains so that the supramolecular aggregation takes place by ionic cross-linking. After the aggregates are formed, addition of a glutaric dialdehyde (GA) solution results in covalent cross-linking of the amine groups of PLL thereby entrapping the HPTS and MNPs in the MFS (Figure 1). The cross-linking by GA is confirmed from the presence of a vibrational band for -C=N- observed at 1642 cm^{-1} in the FT-IR spectrum (Supporting Information, Figure S3). Since the reaction duration influences the extent of cross-linking, the porosity of the spheres can also be controlled.[35]

The hybrid MFS retain their constituents' magnetic and fluorescent properties. As seen in Figure 1 a, the optical image

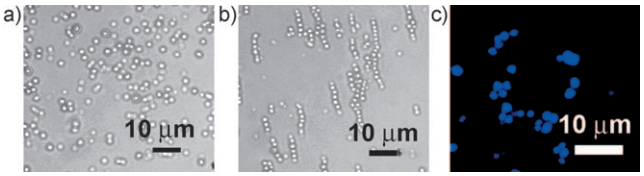

Figure 1. Optical microscopic images of MFS in a) absence and b) presence of an external magnetic field during the analysis; c) Confocal image of the MFS showing the presence of HPTS (blue fluorescence).

clearly reveals that the spheres are well dispersed in water without much specific interaction with neighboring entities. The SEM image (inset of Scheme 1) shows the three-dimensional morphology of the MFS, the sizes of which are in the range of 0.6–1.0 μm. The non-uniform size can be attributed to the inhomogeneity in the sizes of the aggregates formed initially from PLL with MNP and HPTS (Supporting Information, Figure S2). The magnetic properties can be detected by the movement of these MFS in response to an external magnet, as seen under optical microscope (Figure 1 b). The individual MFS are not affected by any residual magnetic field of the incorporated ferrite NPs and hence remain separated. When an external magnetic field is applied, these discrete spheres respond to the magnetic field and assemble themselves as magnetic "worm-like" structures visible under the optical microscope. As soon as the external magnetic field is removed, the aligned chains are disassembled back to individual spherical entities. Analysis by confocal fluorescence microscopy to locate the presence of HPTS in the MFS is shown in Figure 1 c. The MFS are fluorescent and it clearly indicates that the HPTS molecules are encapsulated inside the microspheres (Supporting Information, Figure S4).

Our aim was to prepare 1D aligned hybrid microspheres with the evolution of anisotropic properties from the entrapped magnetic nanoparticles. Based on the response of the MFS to the external magnetic field we designed an experimental set-up (Supporting Information, Figure S5) to construct permanent structures with 1D alignment, in which the spherical aggregates could be cross-linked with GA in presence of a magnetic field. As shown in the set-up, an aqueous GA solution in a microcentrifuge tube is first placed between two parallel magnets. The magnets are separated by a distance of 1.0 cm with a magnetic field of 0.3 T at the point where the GA solution is placed. The aggregates formed by the addition of MNP and HPTS to a PLL solution are then introduced into the GA solution placed under the magnetic field. The alignment of the PLL aggregates containing MNP and HPTS along the direction of the applied magnetic field with simultaneous cross-linking by GA results in 1D aligned MFS structures (Figure 2). The aligned MFS are prepared at various R values (2–20) as shown in the Supporting Information (Figure S6 and Table S1) with $R = 10$ as the optimum condition used for evaluation of their properties.

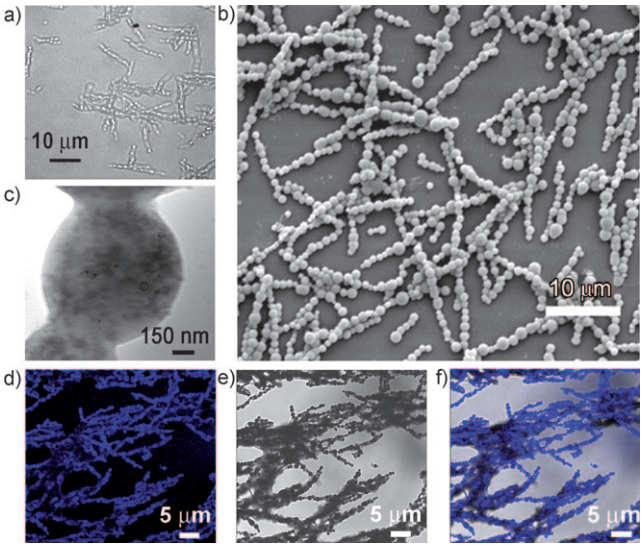

Figure 2. Microscopic images of 1D MFS; a) optical microscopic, b) SEM, c) TEM, d) confocal, e) bright-field, and f) merged confocal and bright-field images of the as-prepared 1D aligned MFS (1D MFS).

Optical microscopy clearly illustrates the 1D shape and beaded-chainlike morphology of the cross-linked hybrid structures (Figure 2 a). Further analysis by SEM (Figure 2 b and inset of Scheme 1) shows that the assembled 1D MFS structures are on average 15 μm long, while the constituent spheres in these have diameters in the range of 0.5–1.2 μm. Each bead has a similarity with the individual MFS structure.

The confocal fluorescence microscopic analysis of the 1D MFS (Figure 2d,f) shows fluorescence emanating from these structures. This clearly indicates that HPTS molecules remain encapsulated in the 1D aligned structure. From the TEM analysis of the 1D MFS structures (Figure 2c) it is apparent that the solid spheres (MFS) are connected to each other to form a 1D structure. It is also seen that the ferrite nanoparticles (MNPs) are entrapped inside the structure. Thermal analysis of the sample (Supporting Information, Figure S7) shows that approximately 15 wt% of ferrite NPs are present in the sample. By taking a higher amount of MNP, the ferrite content in the 1D MFS is further increased to a maximum of 43 wt% (Supporting Information, Figures S8 and S9, Table S1). These MNPs are the key constituents which help the MFS to align under a magnetic field to form 1D aligned structures, while each MFS provides opportunities to integrate functional moieties into the system.

Scheme 1 summarizes the formation of 1D MFS. The first step in which aggregation with the polycation PLL takes place, is the critical step to assemble nanoparticles and other functional molecules into micron-sized spherical structures. Since these spheres contain ferrite nanoparticles, in presence of an external magnet they are magnetized along the field direction. Each spherical aggregate then behaves like a single magnet and thus their magnetic dipole interactions with each other along the external magnetic field leads to the formation of a 1D structure. At the same time the presence of GA cross-links the PLL to form the 1D structure. The GA not only cross-links individual aggregates forming MFS, but also links these spheres together while they are aligned along the magnetic field direction. In contrast, if the GA is added after magnetic alignment of the aggregates it leads to formation of materials without any proper alignment (Supporting Information, Figure S10). This difference may be because the assembled PLL aggregates are destabilized by the movement of constituent magnetic NPs towards the magnet before the action of GA.

The magnetic properties of MFS microspheres processed with and without aligning magnetic field were investigated with a vibrating sample magnetometer (VSM) are shown in the Supporting Information, Figure S11. The magnetic hysteresis curves indicate that the hybrid nanostructures inherit the magnetic properties of the MNPs. The saturation magnetization (M_s) value of the unaligned MFS microspheres (ca. 6.2 emu g^{-1}) is significantly lower than that of the parent citrate-stabilized MNPs (ca. 39 emu g^{-1}). The reduced M_s values are attributed to the non-magnetic constituents, such as HPTS, citrate, and polymer present in the MFS microspheres (Supporting Information, Table S2). However, the aligned MFS microspheres show significant increase in the M_s values (13.1 emu g^{-1}). Taking into account that the MFS microspheres contain 15% Fe_3O_4 (estimated from thermogravimetric analysis (TGA)), this gives a value of 87.8 emu g^{-1}, which is much closer to the corresponding bulk Fe_3O_4 value (92 emu g^{-1} Supporting information, Table S2). The remanence ratio (M_r/M_s), a measure of anisotropy characteristics, determined for the aligned MFS microspheres is about 0.084, which is slightly higher than that of their unaligned counterpart (0.077). This result demonstrates the existence of field-induced particle alignment or anisotropy in the MFS microspheres.[36]

Understanding the origin of the magnetic anisotropy in an assembly of magnetic nanocrystals is an important challenge in the field of nanotechnology. It has implications both at a fundamental and applied level. So to further analyze the magnetic anisotropy characteristics, 1D MFS materials were aligned parallel to each other over a silicon wafer using our experimental set-up (Supporting Information, Figure S5). The drying of the synthesized sample in presence of magnetic field results in alignment of individual 1D MFS along the field direction (Figure 3). The room-temperature magnetic hysteresis curves are presented in Figure 3c. For comparison, the

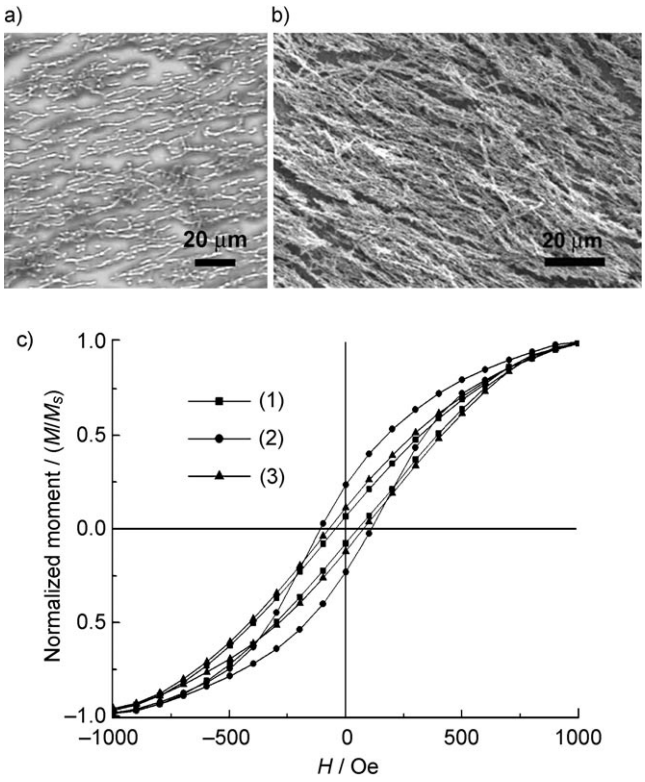

Figure 3. a) Optical microscopy and b) SEM images of the 1D MFS samples dried on a silicon wafer in the presence of a magnetic field; c) magnetic hysteresis curves for the colloidal MFS spheres deposited over silicon wafer without (1) and with aligning field (in-plane (2) and out-of-plane (3) measurements). The magnetic moment is normalized with the maximum saturation value.

1D MFS processed without the aligning field displays relatively poor magnetic properties, that is, in terms of very low remanence (M_r) and coercivity (H_c). In contrast, the 1D MFS processed under the magnetic field shows improved magnetic properties with anisotropy characteristics. The measured H_c values in the in-plane and out-plane are 112 and 72 Oe, respectively. Similarly, the observed remanence ratio, M_r/M_s in the in-plane direction is 0.23; which is 2.3 times higher than that of those observed in the out-plane direction (0.1). The significant increase in the remanence ratio demonstrates the anisotropic characteristics of the aligned 1D

MFS sample. The induced anisotropy is governed by the dipolar interactions of the MNPs inside the microspheres, leading to a complex vortex structure with the magnetic moments aligned parallel to the surface. The dipolar interactions between the microspheres enable their orientation in the resulting 1D MFS. When drop dried under a magnetic field, the 1D MFS chains arrange themselves parallel to each other along the direction of the applied field.

In conclusion, we have demonstrated a hierarchical-assembly process to integrate functional nano- and molecular units that allows the formation of one-dimensional magnetic beaded-chain structures in a colloidal dispersion, the process is driven by an external magnetic field. The aligned 1D particle chains have a magnetic anisotropy which arises from the dipole–dipole interaction of the entrapped MNPs inside the microspheres. This method is rapid, occurs under ambient temperature and in aqueous medium. It should be possible to generalize this method to assemble various other nanoparticles and functional moieties to form hybrid structures and thus facilitate the construction of multifunctional anisotropic materials of interest in various fields.

Experimental Section

A typical synthesis of magnetoresponsive fluorescent microspheres (MFS): A solution of HPTS (75 μL; 1.91 mM) and of Fe_3O_4 (50 μL, 0.05 mg mL^{-1}) in trisodium citrate dispersion (5.36 mM, keeping the ratio *R* of total negative charge on trisodium citrate and HPTS to total positive charge of the PLL at 10) was mixed with poly(L-lysine) (PLL; 25 μL, 2 mg mL^{-1}; Supporting Information, Table S1). The uniformly mixed, slightly turbid solution was injected into a solution of glutaric dialdehyde (GA, 375 μL, 3.33 vol% in water) and allowed to stand undisturbed for 30 min. The MFS were collected with the help of a magnet and washed twice with Millipore water and used for further studies.

Fabrication of aligned 1D MFS: A turbid solution of PLL with HPTS and citrate-functionalized Fe_3O_4 NPs was introduced into a vial containing GA solution placed between two Nd-Fe-B block permanent magnets of similar size and magnetic strength. The two magnets were separated by 1 cm with a spacer (Supporting Information, Figure S5). The aligning magnetic field in the middle of the sample vial was measured to be 0.3 T. The resulted colloidal solution was allowed to stand undisturbed for 30 min. Thus formed 1D aligned MFS were separated from the solution by means of a magnet and washed twice with Millipore water and stored for further studies.

Received: September 8, 2010
Published online: January 11, 2011

Keywords: fluorescent probes · magnetic properties · materials science · nanostructures · self-assembly

[1] R. B. Grubbs, *Nat. Mater.* **2007**, *6*, 553.
[2] S. Sun, *Adv. Mater.* **2006**, *18*, 393.
[3] O. Kriha, M. Becker, M. Lehmann, D. Kriha, J. Krieglstein, M. Yosef, S. Schlecht, R. B. Wehrspohn, J. H. Wendorff, A. Greiner, *Adv. Mater.* **2007**, *19*, 2483.
[4] V. Salgueiriño-Maceira, M. A. Correa-Duarte, *Adv. Mater.* **2007**, *19*, 4131.
[5] R. M. Erb, H. S. Son, B. Samanta, V. M. Rotello, B. B. Yellen, *Nature* **2009**, *457*, 999.
[6] Z. Tang, N. A. Kotov, *Adv. Mater.* **2005**, *17*, 951.
[7] Z. Li, L. Wei, M. Y. Gao, H. Lei, *Adv. Mater.* **2005**, *17*, 1001.
[8] N. Osterman, I. Poberaj, J. Dobnikar, D. Frenkel, P. Ziherl, D. Babic, *Phys. Rev. Lett.* **2009**, *103*, 228301.
[9] E. Braun, Y. Eichen, U. Sivan, G. B. Yoseph, *Nature* **1998**, *391*, 775.
[10] R. Abu-Much, A. Gedanken, *Chem. Eur. J.* **2008**, *14*, 10115.
[11] Y. Lalatonne, J. Richardi, M. P. Pileni, *Nat. Mater.* **2004**, *3*, 121.
[12] M. Z. Wu, Y. Xiong, Y. S. Jia, H. L. Niu, H. P. Qi, J. Ye, Q. W. Chen, *Chem. Phys. Lett.* **2005**, *401*, 374.
[13] G. J. Cheng, D. Romero, G. T. Fraser, A. R. Hight Walker, *Langmuir* **2005**, *21*, 26.
[14] Y. Sahoo, M. Cheon, S. Wang, H. Luo, E. P. Furlani, P. N. Prasad, *J. Phys. Chem. B* **2004**, *108*, 3380.
[15] Z. He, S.-H. Yu, X. Zhou, X. Li, J. Qu, *Adv. Funct. Mater.* **2006**, *16*, 1105.
[16] Y. Xu, J. Yuan, B. Fang, M. Drechsler, M. Müllner, S. Bolisetty, M. Ballauff, A. H. E. Müller, *Adv. Funct. Mater.* **2010**, *20*, 4182.
[17] M. Klokkenburg, C. Vonk, E. M. Claesson, J. D. Meeldijk, B. H. Erne, A. P. Philipse, *J. Am. Chem. Soc.* **2004**, *126*, 16706.
[18] B. D. Korth, P. Keng, I. Shim, S. E. Bowles, C. B. Tang, T. Kowalewski, K. W. Nebesny, J. Pyun, *J. Am. Chem. Soc.* **2006**, *128*, 6562.
[19] S. J. Gong, S. Li, D. Zhang, X. Zhang, C. Liu, Z. Tong, *Chem. Commun.* **2010**, *46*, 3514.
[20] E. Rabani, *J. Chem. Phys.* **2001**, *115*, 1493.
[21] J. F. Banfield, S. A. Welch, H. Zhang, T. T. Ebert, R. L. Penn, *Science* **2000**, *289*, 751.
[22] Z. A. Peng, X. Peng, *J. Am. Chem. Soc.* **2001**, *123*, 1389.
[23] H. Imahori, H. Norieda, H. Yamada, Y. Nishimura, I. Yamazaki, Y. Sakata, S. Fukuzumi, *J. Am. Chem. Soc.* **2001**, *123*, 100.
[24] H. B. Lu, L. Liao, J. C. Li, M. Shuai, Y. L. Liu, *Appl. Phys. Lett.* **2008**, *92*, 093102.
[25] R. K. Rana, V. S. Murthy, J. Yu, M. S. Wong, *Adv. Mater.* **2005**, *17*, 1145.
[26] V. S. Murthy, R. K. Rana, M. S. Wong, *J. Phys. Chem. B* **2006**, *110*, 25619.
[27] V. S. Murthy, J. N. Cha, G. D. Stucky, M. S. Wong, *J. Am. Chem. Soc.* **2004**, *126*, 5292.
[28] M. S. Toprak, B. J. McKenna, M. Mikhaylova, J. H. Waite, G. D. Stucky, *Adv. Mater.* **2007**, *19*, 1362.
[29] D. Patra, A. J. Amali, R. K. Rana, *J. Mater. Chem.* **2009**, *19*, 4017.
[30] A. J. Amali, R. K. Rana, *Chem. Commun.* **2008**, 4165.
[31] K. Kalyanasundaram, *Photochemistry in Microheterogeneous Systems*, Academic Press, Boca Raton, FL, **1987**.
[32] R. Ma, B. Wang, X. Liu, Y. An, Y. Li, Z. He, L. Shi, *Langmuir* **2007**, *23*, 7498.
[33] F. A. Tourinho, R. Franck, R. Massart, *Prog. Colloid Polym. Sci.* **1989**, *79*, 128.
[34] A. J. Amali, R. K. Rana, *Green Chem.* **2009**, *11*, 1781.
[35] M. S. Toprak, B. J. McKenna, J. H. Waite, G. D. Stucky, *Chem. Mater.* **2007**, *19*, 4263.
[36] M. Suda, Y. Einaga, *Angew. Chem.* **2009**, *121*, 1786; *Angew. Chem. Int. Ed.* **2009**, *48*, 1754.

